Low-temperature and high-pressure phase transitions in ferroelectric dabcoHBF$_4$

Low-temperature and high-pressure phase transitions in ferroelectric dabcoHBF$_4$

Marek Szafrański

Faculty of Physics, Adam Mickiewicz University, Umultowska 85, 61-614 Poznań, Poland

E-mail: masza@main.amu.edu.pl

Abstract

NH--N hydrogen bonded ferroelectric dabcoHBF$_4$, $[C_6H_{13}N_2]^+\cdot BF_4^-$, has been studied by dielectric spectroscopy, differential thermal analysis and pyroelectric charge measurement investigations in the low-temperature range between 12 and 300 K, and at elevated hydrostatic pressures up to 1 GPa. The p–T phase diagram has been determined and described. In addition to the known first-order phase transitions at 378 and 153 K, two new structural transitions of continuous type have been revealed, i.e., the transition at 37 K and the pressure-induced one occurring above the triple point situated at 80 MPa and 165 K. Both of these transitions have essentially displacive character and a mechanism related to distortions of the hydrogen bonded polycationic chains, preserving polar properties of the crystal. The possible order–disorder contribution to the transition at 153 K between the ferroelectric phases II and III is discussed in relation to the conformational properties of the dabco cation.

1. Introduction

The crucial role of hydrogen bonds for many processes and potential application of this specific interaction as a tool for use in crystal engineering are still attracting growing interest in the hydrogen bonded structures [1, 2]. Numerous studies have been carried out to describe transformations of hydrogen bonds in OH--O bonded crystals undergoing a ferroelectric–paraelectric phase transition coupled with H disordering [3, 4]. Recently we have demonstrated [5, 6] that ferroelectricity associated with ordering of protons in the bistable hydrogen bonds can also be realized in structures other than the OH--O bonded ones. A newly discovered group of ferroelectric materials consists of monosalts of 1,4 diazabicyclo[2.2.2]octane, $C_6H_{12}N_2$ (denoted as dabco), i.e., dabcoHBF$_4$, dabcoHClO$_4$ and dabcoHReO$_4$. All are ferroelectrics at room temperature, undergoing a ferroelectric–paraelectric phase transition at nearly the same T_C: 378, 377 and 374 K, respectively for dabco
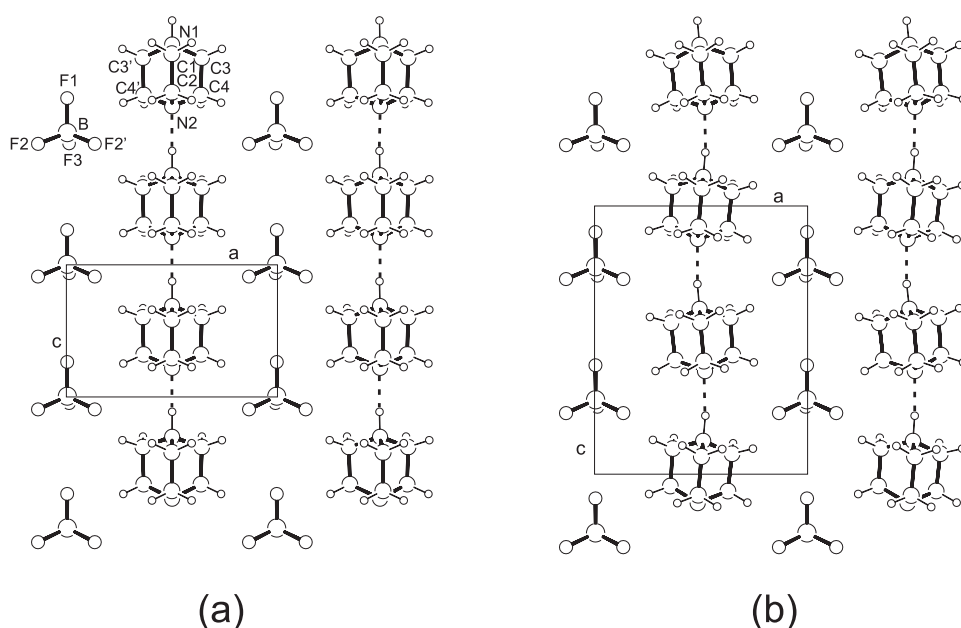
Figure 1. The crystal structure of dabcoHBF$_4$ in the ferroelectric phase II (after [8]), viewed along [010] (a), and the (hypothetical) transformations leading to the doubling of the unit cell parameter *c* in the high-pressure phase V, shown schematically (b).

tetrafluoroborate, perchlorate and perrhenate. The common features of these crystal structures are the chains of the dabco cations linked by the nearly linear NH$^+$--N hydrogen bonds, and the anionic sublattices built from the tetrahedral units (see figure 1(a)). In the ferroelectric phases of the isostructural dabcoHBF$_4$ and dabcoHClO$_4$ the NH$^+$--N bonded chains are polarized, but arranged antiparallel [5, 7, 8], while in dabcoHReO$_4$ a unique parallel arrangement of the chains, resulting in the record spontaneous polarization, is observed [6]. The NH$^+$--N hydrogen bonds in these crystals are all close to 2.85 Å, so they are much longer and thus weaker than their counterparts in the OH--O bonded ferroelectrics. Nevertheless, in the paraelectric phases of dabco salts the acidic protons are disordered [5, 6, 9]. The hopping of the protons between the two sites in the hydrogen bonds is induced by the dynamic disordering of the ions. A coupling of the proton and anion sites, evidenced from crystallographic studies [8], is attended by a coupling of the anionic and protonic motions. This indicates a new possible mechanism for the proton transfers in the hydrogen bonds. A secondary role of the proton itself in the mechanism of the ferroelectric–paraelectric phase transition in the dabco crystals is seen in the positive pressure coefficient dT_c/dp [10] and the weak negative effect of the isotope H/D substitution [5, 11]. These characteristics are clearly different to those observed for KH$_2$PO$_4$-type ferroelectrics. The strictly one-dimensional systems of the hydrogen bonds in the dabco salts are unique among the hydrogen bonded ferroelectrics. This structural feature has multiple consequences for the properties of these materials. The uniaxial relaxor-like behaviour discovered most recently in dabcoHBF$_4$ along [001], perpendicular to the ferroelectric axis [010] of the crystal [12], pertains to the most outstanding. The polar regions embedded in the antiferroelectric matrix are generated due to the proton transfers in the linear NH$^+$--N hydrogen bonds.

Our previous studies [5, 13, 14] have shown that at atmospheric pressure dabcoHBF$_4$ undergoes a sequence of first-order phase transitions:

—phase I($P4/mmm$)—378 K—phase II($Pm2_1n$)—153 K—phase III($Pb2_1a$)—.

The temperature $T_C = 378$ K is the ferroelectric Curie point between the ferroelectric and paraelectric phase, while the transition at $T_{23} = 153$ K occurs between two ferroelectric phases. The present paper is mainly devoted to low-temperature and high-pressure studies of dabcoHBF$_4$. The results provide additional information on the phase situation in this ferroelectric. The pressure-induced effects and the mechanism of phase transitions are discussed in relation to the structural properties of the crystal.

2. Experimental details

The dabcoHBF$_4$ crystals were grown in the ferroelectric phase, at 275 K, by slow evaporation of the saturated aqueous solution. For dielectric measurements at ambient pressure the crystal plates 0.2–0.5 mm thick were cut perpendicular to the main crystallographic directions [100], [010] and [001]. The large faces of the samples were polished and covered with silver paste. Polycrystalline samples prepared in the form of pressed pellets with deposited silver electrodes were used for the high-pressure dielectric measurements.

Complex dielectric permittivity was measured with a Hewlett-Packard 4192A impedance analyser in the frequency range from 10 kHz to 10 MHz at the ac measuring field of 2–5 V cm^{-1}. The temperature was changed at the rate of 0.5–1 K min^{-1}.

The temperature dependence of the spontaneous polarization was measured for a single-domain crystal by the pyroelectric charge method with a Keithley 6514 electrometer. The temperature was changed at a rate of 2 K min^{-1}. A closed-cycle helium cooler CCC1204 was used for the low-temperature dielectric measurements at ambient pressure.

The high-pressure studies were performed by dielectric and differential thermal analysis (DTA; for details see [15]) methods. The sample used in the complex permittivity measurements or the DTA head with the dabcoHBF$_4$ sample were mounted in the high-pressure beryllium bronze cell. A GCA-10 Unipress compressor and helium gas as a pressure transmitting medium were applied for pressure generation in the range from 0.1 MPa to 1 GPa. A manganin gauge ensured pressure calibration with an accuracy of ± 2 MPa.

Calorimetric measurements at ambient pressure were performed by means of DTA in the temperature range from 100 to 300 K. The polycrystalline sample of 62 mg was heated/cooled at a temperature rate ranging from 2 to 5 K min^{-1}. The thermodynamic quantities of the phase transition were determined with an accuracy of 10% as mean values obtained from several DTA runs. The calorimeter was calibrated using indium as a standard substance.

3. Results and discussion

### 3.1. The transition at $T_{23} = 153$ K

Calorimetric studies of dabcoHBF$_4$ revealed a thermal anomaly near $T_{23} = 153$ K related to the structural phase transition between two ferroelectric phases observed earlier [13, 14]. The thermodynamically first-order character of this transition is clearly seen in figure 2 from the shape of the anomaly and its temperature hysteresis. The transition enthalpy, $\Delta H = 0.607$ kJ mol^{-1}, corresponds to the entropy change $\Delta S = 3.97$ J mol^{-1} K^{-1}. The entropy gain can be compared to $R \ln N_2/N_3$, where R is a gas constant and N_2, N_3 are the numbers of configurations in the ferroelectric phases II and III, respectively. The experimental value of ΔS amounts to $R \ln 1.6$ indicating a possible order–disorder contribution to this phase transition. The x-ray structural studies [14] have shown that the transition at T_{23} involves, among other things, conformational changes of the dabco cation: below the transition temperature the cation loses the mirror-plane symmetry assuming a propeller-like conformation. The mutual twists
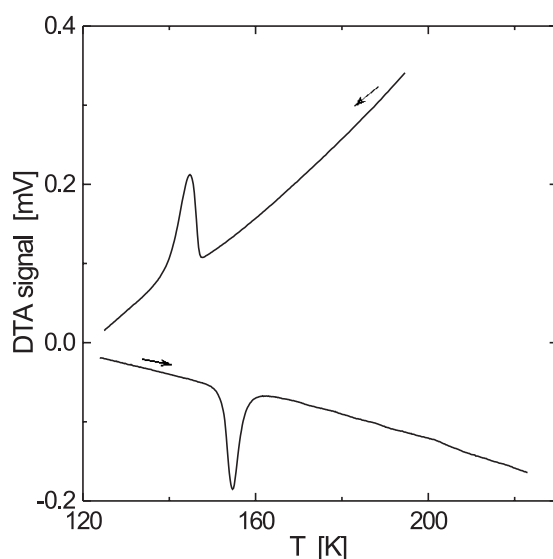
Figure 2. The DTA runs recorded on cooling and heating the polycrystalline dabcoHBF$_4$ sample in the temperature region of the first-order phase transition between phases II and III.

of the cations neighbouring along [100] proceed alternatively clockwise and anticlockwise, leading to the doubling of the unit cell. Therefore, two configurations of the cation must be considered in the phase III. On the other hand, the mirror-plane symmetry of the cation in phase II suggests a single-configuration cationic state above T_{23}. Alternatively, the cation can be disordered in a way that simulates such a symmetry. The mirror-plane symmetry condition could be satisfied by fast transformations of the cation between two oppositely twisted propeller-like conformations or between three conformations: a non-twisted one (with a mirror symmetry plane) and two oppositely twisted propeller-like conformations. The model of threefold conformational disordering of the cation in phase II leads to the configuration entropy change $\Delta S = R \ln 1.5$, which is very close to the experimental value. Although the structural studies do not provide clear evidence of such a disorder in phase II, the anisotropically elongated thermal ellipsoids of C atoms of the dabco cation, observed at low temperature just above T_{23}, could favour the proposed model.

Figure 3(a) shows the low-temperature dependences of the dielectric constant, ε', and dielectric loss, $\tan \delta$, measured at ambient pressure and at 100 kHz electric field applied to the crystal along [100] and [001]. The $\varepsilon'_a(T)$ and $\varepsilon'_b(T)$ scans were very similar; hence the latter was omitted. The jump-wise changes in the dielectric functions at T_{23} are consistent with a first-order character of the transition. It is characteristic that while ε'_a and ε'_b decrease suddenly when the crystal passes to phase III, the transition along [001] is manifested as an increase in ε'_c. Below the transition temperature $\varepsilon'_c(T)$ exhibits a broad anomaly, which is frequency dependent (the dispersion is not shown in figure 3(a); for details see [12]). Moreover, in this direction the transition is also clearly seen in the dielectric loss, distinctly increasing in the low-temperature phase. The unusual anisotropy of the dielectric response of dabcoHBF$_4$ has been ascribed to a short-range ferroelectric order coexisting with a long-range antiferroelectric arrangement of the polycationic chains, and resulting in a one-dimensional relaxor-like behaviour along the [001] direction of the crystal [12]. The strong temperature dependence of ε'_c above 200 K is due to the anionic and protonic jumping between different sites in the crystal lattice. These motions
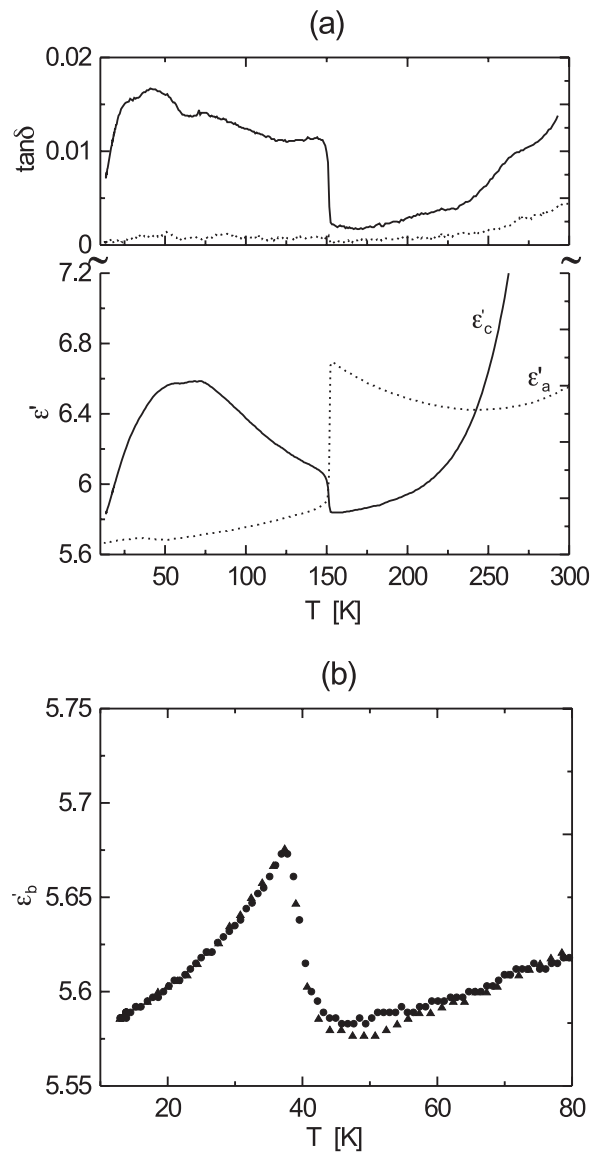
Figure 3. The temperature dependences of ε' and $\tan\delta$ measured for the electric field parallel to [100] and [001] on cooling the crystal (a), and the low-temperature anomaly in $\varepsilon_b'(T)$ measured on cooling (circles) and on heating (triangles) (b). The measuring electric field frequency was 100 kHz.

of charged units contribute exclusively to the permittivity along [001] because their jumps take place between the sites exactly along this direction.

3.2. Low-temperature phase transition

A careful examination of the dielectric data indicates that an additional anomaly in $\varepsilon_a'(T)$ is observable below 50 K (see figure 3(a)). This small singularity also occurs along the
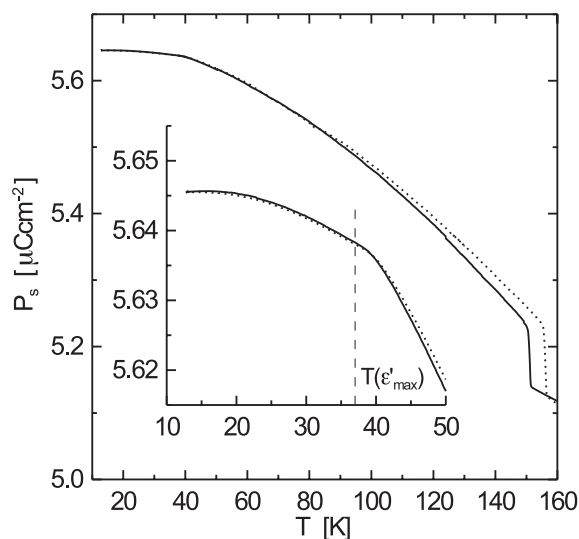
Figure 4. The spontaneous polarization of dabcoHBF$_4$ as a function of temperature measured on cooling (solid curve) and on heating (dotted curve) the crystal. The inset shows the anomalous behaviour of P_s in the vicinity of the dielectric permittivity anomaly at 37 K.

ferroelectric axis [010]. The heating and cooling scans do not show any temperature hysteresis and the anomaly peaks at 37 K, as illustrated in figure 3(b). The anomaly has also been detected in the low-temperature dependence of the spontaneous polarization of the crystal. The $P_s(T)$ plots in figure 4 demonstrate the step-wise change associated with the first-order phase transition at T_{23}, and the subtle anomalous changes around 37 K. The results of dielectric and pyroelectric measurements strongly suggest that dabcoHBF$_4$ undergoes a continuous phase transition at $T_{34} = 37$ K, between the ferroelectric phase III and the low-temperature ferroelectric phase IV.

3.3. Pressure-induced phase transition

At elevated pressures the dielectric anomaly associated with the transition between phases II and III was shifted to higher temperatures, as seen in figure 5(a). For high-pressure studies we used polycrystalline samples; thus the spatially averaged dielectric functions were examined. Nevertheless, it is evident from the results obtained that very modest pressure induces a new phase in dabcoHBF$_4$, denoted hereafter as phase V. The transition, indicated by the vertical arrows in figure 5(a), is associated with the small but evident anomalous changes in the real part of the dielectric constant, and does not affect the dielectric loss (see figure 5(b)). Accordingly, it is reasonable to assume that it has a non-ferroelectric nature. As can be seen from figures 5(a) and (b), the new anomaly is manifested as a progressive change of $\varepsilon'(T)$ with no thermal hysteresis between the cooling and heating cycles, indicating a continuous character of the phase transition. The differences in magnitude of ε' between different temperature scans arise from the domain structure contribution, which depends of the thermal history of the sample. To get more information on the pressure-induced phase transition we performed high-pressure calorimetric measurements. The DTA runs have shown only the presence of one thermal anomaly related to the first-order phase transition between the phases II and III, with no trace of an additional transition at elevated pressures. This indicates that the thermal effect associated
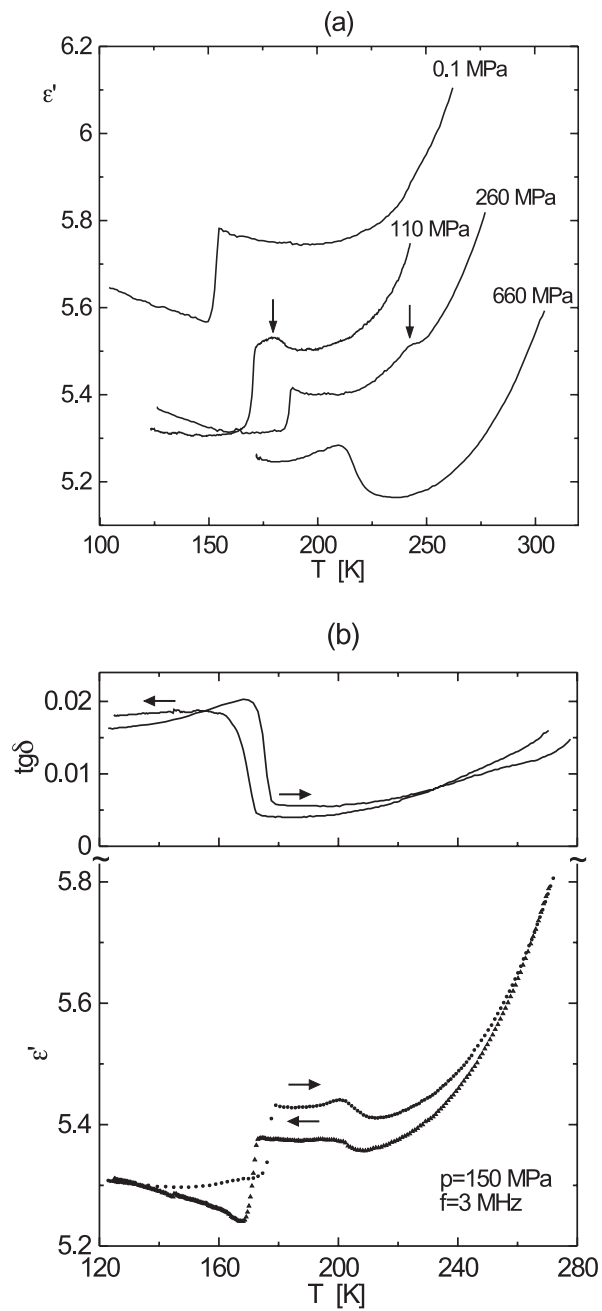
Figure 5. The $\varepsilon'(T)$ dependences measured at the electric field frequency of 5 MHz for the polycrystalline dabcoHBF$_4$ sample under several pressures (a) and the heating/cooling scans of ε' and $\tan \delta$ across the transitions II–V and V–III, at 150 MPa (b). The vertical arrows mark the pressure-induced anomaly.

with the pressure-induced transition have to be relatively small. Therefore we conclude that this transition is prevailingly of displacive type. According to group–subgroup relations [16],
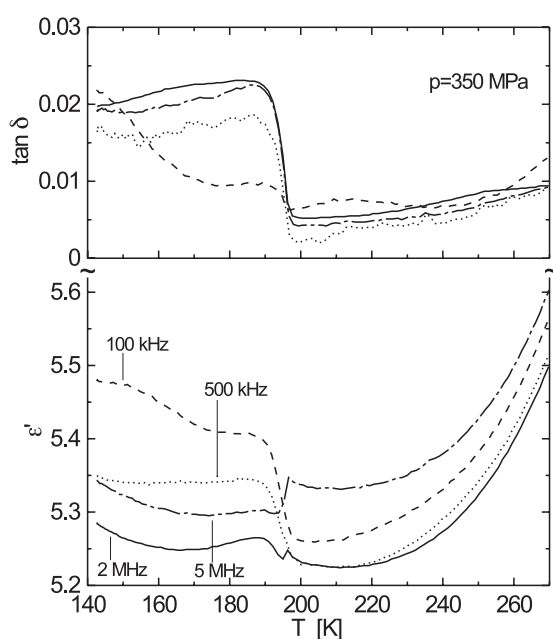
Figure 6. The temperature and frequency dependences of ε' and $\tan\delta$ at the elevated pressure of 350 MPa.

and the non-ferroelectric and continuous character of the transition, two possibilities for the crystal symmetry change can be expected, namely $Pm2_1n \rightarrow Pm2_1n$ and $Pm2_1n \rightarrow Pn2_1a$, both involving a doubling of the unit cell. The latter case seems to be more probable because the symmetry of the $Pn2_1a$ space group was recently found for the low-temperature phase of isostructural dabcoHClO$_4$ [17], at ambient pressure. Analogously, the doubling of the unit cell in dabcoHBF$_4$ could result from the small antiphase tilts of the dabcoH$^+$ cations with respect to (100), as schematically illustrated in figure 1(b). The ClO$_4^-$ anions are slightly larger than BF$_4^-$ and thus exert an additional internal pressure on the polycationic sublattice. The application of hydrostatic pressure to the dabcoHBF$_4$ structure can modify the cation–anion interplay in a similar way to the increase of the cation size, leading to distortions of the hydrogen bonded framework. Indeed, a preliminary high-pressure x-ray single-crystal study [18] has shown the occurrence of a new phase in dabcoHBF$_4$ at elevated pressures, which was manifested by the presence of superstructure reflections.

Noteworthy is the pressure effect on the dielectric response of the crystal, resulting in an inversion of the dielectric anomaly associated with the first-order phase transition at T_{23}. As seen in figure 5(a), the transition dielectric increment $\Delta\varepsilon'$ (i.e., the difference in ε' between phases II and III) diminishes with increasing pressure, and finally its sign changes. For lower frequencies this effect was observed at lower pressures as can be deduced from the results shown in figure 6. The frequency dispersion in $\varepsilon'(T)$ and $\tan\delta(T)$, resulting from the relaxor-like behaviour of the crystal, is very sensitive to the applied pressure. In relaxor systems high pressure can affect the length of correlation among the polar nanoclusters as well as the slowing down of their dynamic fluctuations [19]. Both of these effects can contribute to the pressure-induced changes in the dielectric functions of dabcoHBF$_4$.

3.4. p–T phase diagram

The results of the high-pressure measurements are summarized in figure 7 illustrating the temperature–pressure phase relations in dabcoHBF$_4$. The boundary between paraelectric
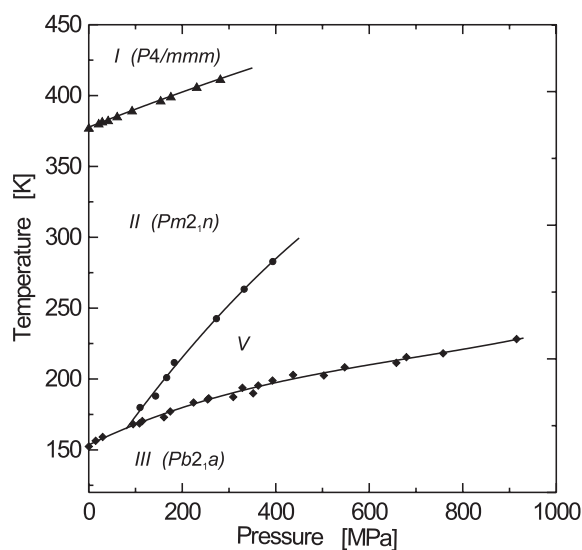
Figure 7. The p–T phase diagram of dabcoHBF$_4$. The solid curves represent the best fits of the polynomial functions of pressure to the experimental points.

phase I and ferroelectric phase II is weakly non-linear and is well described by a quadratic function of pressure, as reported earlier [10]. Non-linear p–T dependences are also observed for the transitions between ferroelectric phases II, III and V. All the transition lines can be fitted with polynomial functions of pressure of the following general form:

$$T_{tr} = T_0 + \alpha p + \beta p^2 + \gamma p^3, \tag{1}$$

where T_0 denotes the transition temperature extrapolated to ambient pressure, and α, β, γ are the coefficients fitted to the experimental data. The parameters describing the equilibrium lines are collected in table 1. Using these data the triple point in the p–T phase diagram of dabcoHBF$_4$ was estimated at 80 MPa and 165 K. For the first-order phase transition the equilibrium line satisfies the Clausius–Clapeyron equation:

$$\frac{dT_{tr}}{dp} = \frac{\Delta V}{\Delta S}, \tag{2}$$

where ΔV and ΔS are the transition volume and entropy change, respectively. At atmospheric pressure the volume of the crystal unit cell, estimated from x-ray dilatometric studies [14], diminishes abruptly by about 1 Å^3 per formula unit when the crystal transforms to the low-temperature phase III. Taking into account the transition entropy change derived from our present calorimetric measurements we obtain the slope $dT_{23}/dp = 0.152$ K MPa^{-1}, in good agreement with the one extracted directly from the phase diagram, 0.159 K MPa^{-1} (see also table 1).

4. Conclusions

DabcoHBF$_4$ belongs to a new group of ferroelectric NH$^+$--N bonded crystals, which are characterized by exceptionally simple structure based on the one-dimensional polycationic chains. The structure is strongly stabilized by hydrogen bonds, but on the other hand the NH$^+$--N bonds ensure a certain structural flexibility, resulting in a sequence of phase transitions.

Table 1. The parameters resulting from the best fitting of the equation (1) to the experimental data shown in figure 7.

Transition line	T_0 (K)	α (K MPa^{-1})	β (10^{-5} K MPa^{-2})	γ (10^{-8} K MPa^{-3})
I–II	377.7	0.13	2.99	0
II–V	127.5	0.484	22.6	0
II–III and V–III	153.5	0.159	−15.2	7.35

The transitions preserve, however, the general structural features of the crystal, which retains its polar properties across the four crystalline phases. The paraelectric/ferroelectric phase transition is driven by the ordering of the ions and protons, but also involves a significant displacive factor, giving rise to the spontaneous polarization of the crystal [5, 10]. The transition at T_{23} between two ferroelectric phases II and III is induced by the onset of conformational transformations in the cations [14]. The results of the present calorimetric study indicate an order–disorder contribution to this transition. A model of the dynamical three-conformational disorder of the cation in phase II has been proposed to rationalize the transition mechanism. However, the behaviour of the protons in the bistable NH$^+$--N hydrogen bonds and their role in the transition mechanism are still unclear [14], and the problem requires further study by other methods, including neutron diffraction studies. While the first-order phase transitions at T_C and T_{23} contain both order–disorder and displacive contributions, the low-temperature transition at $T_{34} = 37$ K and the pressure-induced transition are continuous and essentially of displacive nature, related most probably to the subtle transformations in the hydrogen bonded polycationic sublattice and small changes in the crystal packing.

Acknowledgments

References

[1] Jeffrey G A 1997 *Introduction to Hydrogen Bonding* (Oxford: Oxford University Press)
[2] Desiraju G R 1989 *Crystal Engineering: The Design of Organic Solids* (New York: Elsevier)
[3] Jona F and Shirane G 1993 *Ferroelectric Crystals* (New York: Dover)
[4] Tomaszewski P 1992 *Phase Transit.* **38** 127
[5] Katrusiak A and Szafrański M 1999 *Phys. Rev. Lett.* **82** 576
[6] Szafrański M, Katrusiak A and McIntyre G J 2002 *Phys. Rev. Lett.* **89** 215507
[7] Głowiak T, Sobczyk L and Grech E 1975 *Chem. Phys. Lett.* **36** 106
[8] Katrusiak A, Ratajczak-Sitarz M and Grech E 1999 *J. Mol. Struct.* **474** 135
[9] Katrusiak A 2000 *J. Mol. Struct.* **552** 159
[10] Szafrański M and Katrusiak A 2000 *Chem. Phys. Lett.* **318** 427
[11] Żogał O J, Galewski Z, Grech E and Malarski Z 1985 *Mol. Phys.* **56** 673
[12] Szafrański M and Katrusiak A 2004 *J. Phys. Chem.* B submitted
[13] Przesławski J and Szafrański M 2002 *Ferroelectrics* **269** 45
[14] Budzianowski A, Katrusiak A and Szafrański M 2004 in preparation
[15] Szafrański M, Czarnecki P, Katrusiak A and Habryło S 1992 *Solid State Commun.* **82** 277
[16] Stokes H T and Hatch D M 1988 *Isotropy Subgroups of the 230 Crystallographic Space Groups* (Singapore: World Scientific)
[17] Budzianowski A and Katrusiak A 2004 in preparation
[18] Katrusiak A and Dera P 2001 private communication
[19] Samara G A 2003 *J. Phys.: Condens. Matter* **15** R367